RESEARCH ARTICLE

A Noncanonical Autophagy Pathway Restricts *Toxoplasma gondii* Growth in a Strain-Specific Manner in IFN-γ-Activated Human Cells

Elizabeth M. Selleck,[a] Robert C. Orchard,[b] Kara G. Lassen,[c] Wandy L. Beatty,[a] Ramnik J. Xavier,[c,d] Beth Levine,[e] Herbert W. Virgin,[b] L. David Sibley[a]

Department of Molecular Microbiology,[a] Department of Pathology and Immunology,[b] Washington University School of Medicine, St. Louis, Missouri, USA; Broad Institute of MIT and Harvard, Cambridge, Massachusetts, USA[c]; Gastrointestinal Unit and Center for the Study of Inflammatory Bowel Disease, Massachusetts General Hospital and Harvard Medical School, Boston, Massachusetts, USA[d]; Center for Autophagy Research, Department of Internal Medicine, Department of Microbiology and Howard Hughes Medical Institute, University of Texas Southwestern Medical Center, Dallas, Texas, USA[e]

ABSTRACT **A core set of autophagy proteins is required for gamma interferon (IFN-γ)-mediated clearance of *Toxoplasma gondii* in the mouse because of their control of several downstream effectors, including immunity-related GTPases (IRGs) and guanylate-binding proteins (GBPs). However, these effectors are absent (i.e., IRGs) from or nonessential (i.e., GBPs) in IFN-γ-activated human cells, raising the question of how these cells control parasite replication. Here, we define a novel role for ubiquitination and recruitment of autophagy adaptors in the strain-specific control of *T. gondii* replication in IFN-γ-activated human cells. Vacuoles containing susceptible strains of *T. gondii* became ubiquitinated, recruited the adaptors p62 and NDP52, and were decorated with LC3. Parasites within LC3-positive vacuoles became enclosed in multiple layers of host membranes, resulting in stunting of parasite replication. However, LC3-positive *T. gondii*-containing vacuoles did not fuse with endosomes and lysosomes, indicating that this process is fundamentally different from xenophagy, a form of autophagy involved in the control of intracellular bacterial pathogens. Genetic knockout of ATG16L or ATG7 reverted the membrane encapsulation and restored parasite replication, indicating that core autophagy proteins involved in LC3 conjugation are important in the control of parasite growth. Despite a role for the core autophagy machinery in this process, upstream activation through Beclin 1 was not sufficient to enhance the ubiquitination of *T. gondii*-containing vacuoles, suggesting a lack of reliance on canonical autophagy. These findings demonstrate a new mechanism for IFN-γ-dependent control of *T. gondii* in human cells that depends on ubiquitination and core autophagy proteins that mediate membrane engulfment and restricted growth.**

IMPORTANCE **Autophagy is a process of cellular remodeling that allows the cell to recycle senescent organelles and recapture nutrients. During innate immune responses in the mouse, autophagy is recruited to help target intracellular pathogens and thus eliminate them. However, the antimicrobial mediators that depend on autophagy in the mouse are not conserved in humans, raising the issue of how human cells control intracellular pathogens. Our study defines a new pathway for the control of the ubiquitous intracellular parasite *T. gondii* in human cells activated by IFN-γ. Recruitment of autophagy adaptors resulted in engulfment of the parasite in multiple membranes and growth impairment. Although susceptible type 2 and 3 stains of *T. gondii* were captured by this autophagy-dependent pathway, type 1 strains were able to avoid entrapment.**

Received 11 July 2015 **Accepted** 12 August 2015 **Published** 8 September 2015

Citation Selleck EM, Orchard RC, Lassen KG, Beatty WL, Xavier RJ, Levine B, Virgin HW, Sibley LD. 2015. A noncanonical autophagy pathway restricts *Toxoplasma gondii* growth in a strain-specific manner in IFN-γ-activated human cells. mBio 6(5):e01157-15. doi:10.1128/mBio.01157-15.

Invited Editor Jon P. Boyle, University of Pittsburgh **Editor** John C. Boothroyd, Stanford University

Address correspondence to L. David Sibley, sibley@wusm.wustl.edu.

Toxoplasma gondii is an obligate intracellular parasite that infects a wide range of mammalian hosts (1) and frequently causes infections in humans (2). Humans are infected either through the ingestion of oocysts shed into the environment by their definitive host, the cat, or through ingestion of tissue cysts from infected animals (1). In North America and Europe, three clonal strains of *T. gondii* predominate, referred to as type 1, 2, and 3 strains (3). As a zoonotic infection, the distribution of strains in humans should mirror that of the animals by which they are infected. However, despite the fact that type 2 and 3 *T. gondii* strains are both common in food animals, only type 2 strains are prevalent in human infections, whereas type 3 strains are extremely rare (4, 5). Conversely, type 1 strains are rare in animals yet elevated in human infections, at least among some cohorts (4). This differential strain distribution suggests that there are strain-specific differences between the infection of humans and that of animals, although the factors underlying these different outcomes remain unclear.

T. gondii tachyzoites actively invade their host cell, invaginating the host cell plasma membrane to create a compartment that is permissive for parasite replication (6) while excluding most host membrane proteins from the surrounding parasitophorous vacuole membrane (PVM) (7, 8). Within this niche, the parasite replicates asexually to high numbers before lysing the host cell by egress, which is an active, parasite-driven process (9). The parasite-containing vacuole does not fuse with endosomes or ly-

sosomes; hence, the PVM remains LAMP-1 negative (8, 10–12). Although *T. gondii* is able to survive in naive macrophages, activation with gamma interferon (IFN-γ) leads to the upregulation of a variety of resistance factors that are important for control in mice, including the immunity-related GTPases (IRGs), guanylate-binding proteins (GBPs), reactive oxygen species, and nitric oxide (13, 14). Recruitment of IRGs (15–17) and GBPs (18–20) to PVs surrounding susceptible *T. gondii* strains leads to clearance, a process countered by parasite virulence factors that are associated primarily with virulent type 1 strains (21).

Activation by IFN-γ also leads to control of parasite replication in human cells, although the mechanism is less well understood. Humans lack the majority of the IRGs, including those that have been shown to localize to the PVM in mouse cells (13, 14). Additionally, deletion of a cluster of GBPs did not affect the ability of IFN-γ-activated human HAP1 cells to control the replication of *T. gondii* (22). Instead, other studies have shown that IFN-γ treatment of human cells can lead to growth restriction due to tryptophan depletion (23) and induction of cell death and premature egress (24). However, neither of these mechanisms operates in all cell types, suggesting the presence of multiple overlapping pathways for IFN-γ-mediated control of *T. gondii* in human cells. Additionally, it has been shown that the ligation of CD40 on the surface of hematopoietic and nonhematopoietic cells is able to eliminate intracellular *T. gondii* in an autophagy-dependent manner (25, 26), although this mechanism is not dependent on activation by IFN-γ (27).

Macroautophagy is the process by which a cell digests and recycles cytoplasmic contents, including protein aggregates, damaged organelles, and intracellular organisms (28). The trafficking of IRGs and GBPs to the PVM in mouse cells depends on a subset of autophagy (Atg) proteins, including Atg5, Atg12, and Atg16L1, but not the upstream activators of canonical autophagy (22, 29, 30). In mouse cells, the absence of these core Atg proteins results in the aggregation of IRGs (15, 30) and GBPs (19, 31), and thus they are not available for recruitment to the PVM. During canonical autophagy, the double-membrane-bound autophagosome normally goes on to fuse with LAMP-1-positive lysosomes (28). However, following the delivery of IRGs and GBPs to the *T. gondii*-containing PVM, the vacuole does not become LAMP-1 positive but instead is vesiculated and ruptures, resulting in the death of the parasite (29, 30, 32). Thus, control of *T. gondii* in IFN-γ-activated mouse cells does not rely on the downstream degradative functions of autophagy (29).

Recently, a modification of the autophagy pathway has been appreciated as an important arm of cell-autonomous immunity to intracellular bacteria (28, 33). Known as xenophagy, this process targets bacteria that reside within membrane-bound vacuoles, including *Listeria monocytogenes*, *Salmonella enterica* serovar Typhimurium, and group A *Streptococcus* (34–37). Targeting by xenophagy begins with permeation of the bacterium-containing vacuole, followed by ubiquitination and recruitment of autophagy adaptor proteins, including p62, NDP52, and optineurin, leading to the recruitment of LC3 and the formation of an autophagosome. The autophagosome then fuses with LAMP-1-positive lysosomes, and the targeted microbe is degraded (28, 35).

Here, we examined whether xenophagy is also involved in the control of *T. gondii* growth in IFN-γ-activated human cells and if there are strain-dependent differences in susceptibility to this pathway. Additionally, we wanted to determine if autophagy pathway proteins are required for IFN-γ-dependent growth restriction of *T. gondii* in human cells. We found that core ATG proteins are important in the ability of IFN-γ-activated human cells to restrict the growth of *T. gondii*. Importantly, this process occurs independently of fusion with endosomes or lysosomes and is not enhanced by the induction of upstream activation of autophagy, indicating that it differs from both autophagy and xenophagy.

RESULTS

Autophagy adaptors are recruited in a strain-specific manner to *T. gondii* in human cells. To determine whether proteins in the xenophagy pathway are recruited to *T. gondii*-containing parasitophorous vacuoles (PVs) in human cells, we localized ubiquitin, p62, NDP52, and LC3 by quantitative immunofluorescence after infection. Representative strains of type 1 (GT-1), 2 (PTG), and 3 (VEG) parasites were used to compare recruitment in IFN-γ-activated HeLa cells examined at 6 h postinfection. Type 1 PVs were largely able to prevent the accumulation of ubiquitin, as few PVs showed appreciable levels of staining of the vacuole (Fig. 1A). However, many type 2 and 3 PVs were intensely stained with antibodies to ubiquitin. This pattern of type 1 parasites preventing recruitment and accumulation of ubiquitin held true for the other autophagy adaptors p62 and NDP52 (Fig. 1B and C), while again type 2 and 3 strains showed many PVs with high levels of host protein accumulation. LC3 was also recruited to high levels to type 2 and 3 PVs and largely excluded from type 1 PVs (Fig. 1D). Visual assessment of PVs stained for the autophagy adaptors showed that most type 1 PVs were negative for ubiquitin, while a large percentage of type 2 and 3 PVs were positive (Fig. 1E and F). This pattern held true for the other autophagy adaptors p62 and NDP52 and for LC3, with a larger percentage of type 2 and 3 than type 1 parasites positive (Fig. 1E and F). The recruitment of ubiquitin, p62, NDP52, and LC3 depended on prior activation with IFN-γ (Fig. 1G and H) but did not depend on the presence of known parasite virulence factor ROP18, ROP17, or ROP5, inasmuch as deletion of these factors in a type 1 background did not alter recruitment (see Fig. S1A in the supplemental material). Collectively, these data show that proteins associated with the autophagy pathway accumulated on PVs in a strain-dependent manner in IFN-γ-activated human cells.

Autophagy adaptors colocalize on parasite-containing vacuoles. To determine if *T. gondii* PVs are sequentially targeted by ubiquitin and then other members of the xenophagy pathway, we colocalized ubiquitin with the autophagy adaptors p62, NDP52, and LC3 on PVs. In IFN-γ-activated HeLa cells, ubiquitin showed a similar pattern of colocalization with p62, NDP52, and LC3. For ubiquitin and p62, the majority of the PVs (72.7%) were positive for both ubiquitin and p62, while 23.7% were positive for ubiquitin alone and no PVs were singly positive for p62 (Fig. 2A and B). A similar pattern was seen with NDP52 and LC3 (Fig. 2C to F), with between 28 and 30% of the PVs positive for ubiquitin alone, while the majority were positive for both ubiquitin and NDP52 or LC3. This pattern of staining is consistent with a model where ubiquitin is recruited to the vacuole first, leading to subsequent targeting by the other autophagy adaptors and finally recruitment of LC3. We also colocalized the autophagy adaptors NDP52 and p62. These proteins often completely colocalized but in some cases were distinct (Fig. 2H). Additionally, we colocalized p62 and LC3 (Fig. 2J) on PVs. As anticipated, about 90% of the PVs were

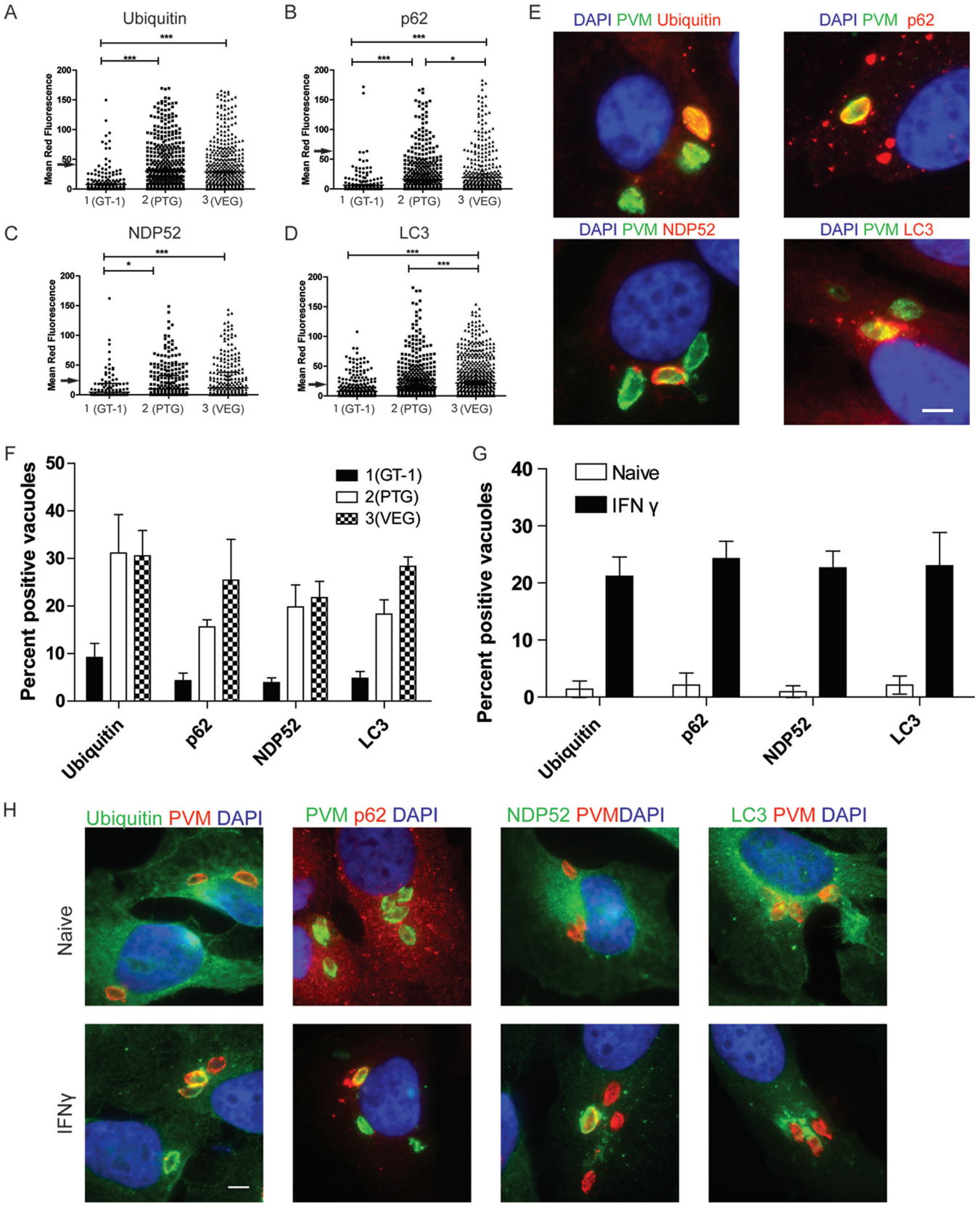

FIG 1 Recruitment of autophagy adaptors to intracellular *T. gondii*. (A to D) Quantification of recruitment of autophagy adaptors to type 1 (GT-1), 2 (PTG), or 3 (VEG) *T. gondii* in HeLa cells activated for 24 h with IFN-γ prior to infection and analyzed at 6 h postinfection. Data points represent the mean red fluorescence of the respective host markers in a ROI overlapping the *T. gondii* vacuole. Arrowheads indicate the mean red fluorescence value of 90% of visually

(Continued)

positive for both NDP52 and p62 (Fig. 2G) and a similar pattern was seen with p62 and LC3 (Fig. 2I).

Canonical autophagy culminates in the fusion of the autophagosome with the LAMP-1-positive lysosomes, forming an autophagolysosome and thereby degrading the material within the autophagosome (28). To determine if *T. gondii*-containing PVs in human cells follow a similar route, we colocalized ubiquitin, LC3, and LAMP-1 in IFN-γ-activated HeLa cells at 6 h postinfection. Surprisingly, we found that nearly all of the PVs that were positive for ubiquitin remained negative for LAMP-1 staining (Fig. 2K and L). The few PVs that were positive for LAMP-1 showed a very distinctive, smooth, uniform, parasite-shaped rim of staining (see Fig. S2 in the supplemental material); hence, we are confident that we would have readily detected this staining if it were prevalent. Similarly, a very small proportion of LC3-positive PVs, as detected in HeLa cells expressing green fluorescent protein (GFP)-LC3, were also positive for LAMP-1 (Fig. 2M and N). Together, these findings demonstrate that in IFN-γ-activated human cells, *T. gondii* is targeted by a set of proteins similar to that which targets other intracellular bacteria undergoing xenophagy. However, the vast majority of ubiquitin-positive PVs do not fuse with lysosomes, indicating a unique pathway of trafficking for intracellular *T. gondii.*

PVs are enveloped in multiple membranes in IFN-γ-activated human cells. Intracellular pathogens targeted by ubiquitin and autophagy adaptors are often enclosed in canonical double-membrane structures (38, 39). We examined the ultrastructural features of *T. gondii* PVs at 6 h postinfection in HeLa cells, conditions under which we saw recruitment of ubiquitin, p62, NDP52, and LC3 in an IFN-γ-dependent manner. In naive cells, *T. gondii* PVs were surrounded by a smooth, intact PVM (arrowhead in Fig. 3A). In IFN-γ-activated cells, but not naive cells, a proportion of the PVs were surrounded by multiple membranes that enveloped the *T. gondii* PV within multiple cisternae. These wrapped PVs often appeared to encapsulate a portion of the host cytosol within them (Fig. 3B and C). To examine whether these enveloped PVs were decorated with LC3, we performed cryo-immuno-electron microscopy (cryo-immuno-EM) to localize LC3 in naive and IFN-γ-activated HeLa cells. We compared the distribution of constitutively expressed GFP-LC3 HeLa cells infected with type 3 (VEG) parasites at 6 h postinfection. In naive cells, GFP-LC3 was seen diffusely in the infected cell, with occasional membranous clusters consistent with a low level of autophagy; however, LC3 did not concentrate near the PV (Fig. 4A). In contrast, in IFN-γ-activated cells, large accumulations of GFP-LC3 were seen on the multiple membranes surrounding the PV (Fig. 4B). The accumulation of membranes containing LC3 is consistent with a model where susceptible *T. gondii* PVs are contained within autophagosome-like structures in IFN-γ-activated cells. However, these LC3-positive vacuoles did not become LAMP-1 positive, as shown by double immuno-EM labeling (Fig. 4C). The number of membranes wrapping *T. gondii* PVs was variable: in some cases, the PVM was engulfed by a double-membrane layer, consistent with autophagy, while in other cases, several layers of host membranes, and entrapped cytosol, surrounded the PV (Fig. 4).

Parasite growth is stunted in vacuoles positive for ubiquitin or p62. To assess the functional consequence of the targeting of PVs by xenophagy, we examined the replication of type 3 strain parasites within PVs that were either positive or negative for ubiquitin or p62. *T. gondii* divides by binary fission every 6 to 8 h, and as expected, ubiquitin-negative PVs showed a range of numbers of parasites per vacuole, with ~40% having four or more parasites by 24 h (Fig. 5A and B). In contrast, growth in ubiquitin-positive PVs was significantly impaired, with ~85% having only one or two parasites per vacuole (Fig. 5A). The restriction of growth of ubiquitin-positive PVs was not dependent on the degradation of tryptophan, as supplementation with exogenous tryptophan did not change the replication of ubiquitin-positive PVs (see Fig. S5A in the supplemental material). Similarly, p62-negative PVs showed replication consistent with normal growth kinetics, with ~36% of the PVs containing four or more parasites. Alternatively, p62-positive PVs were significantly restricted, with a great majority, ~95%, containing one or two parasites (Fig. 5C and D). Despite being restricted in growth, type 3 parasites were not cleared from IFN-γ-activated cells (see Fig. S5B). To assess the functional consequences of ubiquitin recruitment to other parasite strains, we determined the percentage of parasites that were positive for ubiquitin over time, as well as parasite replication at 24 h postinfection. Type 2 and 3 strains had a significantly higher percentage of PVs positive for ubiquitin than did type 1 parasites at 6 h postinfection (Fig. 5E). At 24 h postinfection, the percentage of ubiquitin-positive parasites decreased in all vacuoles; however, ~10% of the type 2 and 3 vacuoles remained positive while the type 1 parasites were nearly completely negative (Fig. 5E). Importantly, parasites from all of the strains that were positive for ubiquitin were stunted in their replication, while parasites that were negative for ubiquitin replicated normally (Fig. 5F). Together,

Figure Legend Continued

determined positive vacuoles. Each value is the mean ± SEM of three experiments (***, $P \leq 0.001$; *, $P \leq 0.05$; Kruskal-Wallis test). (E) Immunofluorescence localization of ubiquitin, p62, NDP52, or LC3 to the PVM in HeLa cells activated with 5 ng/ml IFN-γ at 6 h postinfection with type 3 (VEG) parasites. Ubiquitin was localized with mouse MAb FK2, followed by anti-mouse IgG conjugated to Alexa Fluor 594 (red). p62 was localized with a guinea pig polyclonal antibody, followed by anti-guinea pig IgG conjugated to Alexa Fluor 594 (red). NDP52 was localized with a rabbit polyclonal antibody, followed by anti-rabbit IgG conjugated to Alexa Fluor 594 (red). LC3 was localized with a rabbit polyclonal antibody, followed by Alexa Fluor 594 (red). *T. gondii* PVM was localized with either a rabbit polyclonal antibody to GRA7, followed anti-rabbit IgG conjugated to Alexa Fluor 488 (green), or mouse MAb tg17-113 to GRA5, followed by anti-mouse IgG conjugated to Alexa Fluor 488 (green). Nuclei were stained with 4′,6-diamidino-2-phenylindole (DAPI) (blue). Scale bar, 5 μm. (F) Visual assessment of the percentage of host marker-positive *T. gondii* PVs from images used to collect the data shown in panels A to D. Each value is the mean ± SEM of three experiments. (G) Quantification of recruitment of autophagy proteins to type 3 (VEG) parasites in naive or IFN-γ-activated HeLa cells at 6 h postinfection by fluorescence microscopy. There were two experiments and a total of six coverslips. Each value is the mean ± SD. (H) Immunofluorescence images of HeLa cells infected with type 3 (VEG) parasites at 6 h postinfection. HeLa cells were activated with 5 ng/ml IFN-γ. Ubiquitin was localized with mouse MAb FK2, p62 was localized with a guinea pig polyclonal antibody, NDP52 was localized with a rabbit polyclonal antibody, and LC3 was localized with a rabbit polyclonal antibody, followed by secondary antibodies conjugated to Alexa Fluor 488 (green) or 594 (red), as indicated. *T. gondii* PVM was localized with either a rabbit polyclonal antibody to GRA7 or mouse MAb tg17-113 to GRA5, with the opposite antibody species to the host marker, followed by anti-mouse IgG conjugated to Alexa Fluor 488 (green) or 549 (red). Nuclei were stained with DAPI. Scale bar, 5 μm. See also Fig. S1 in the supplemental material.

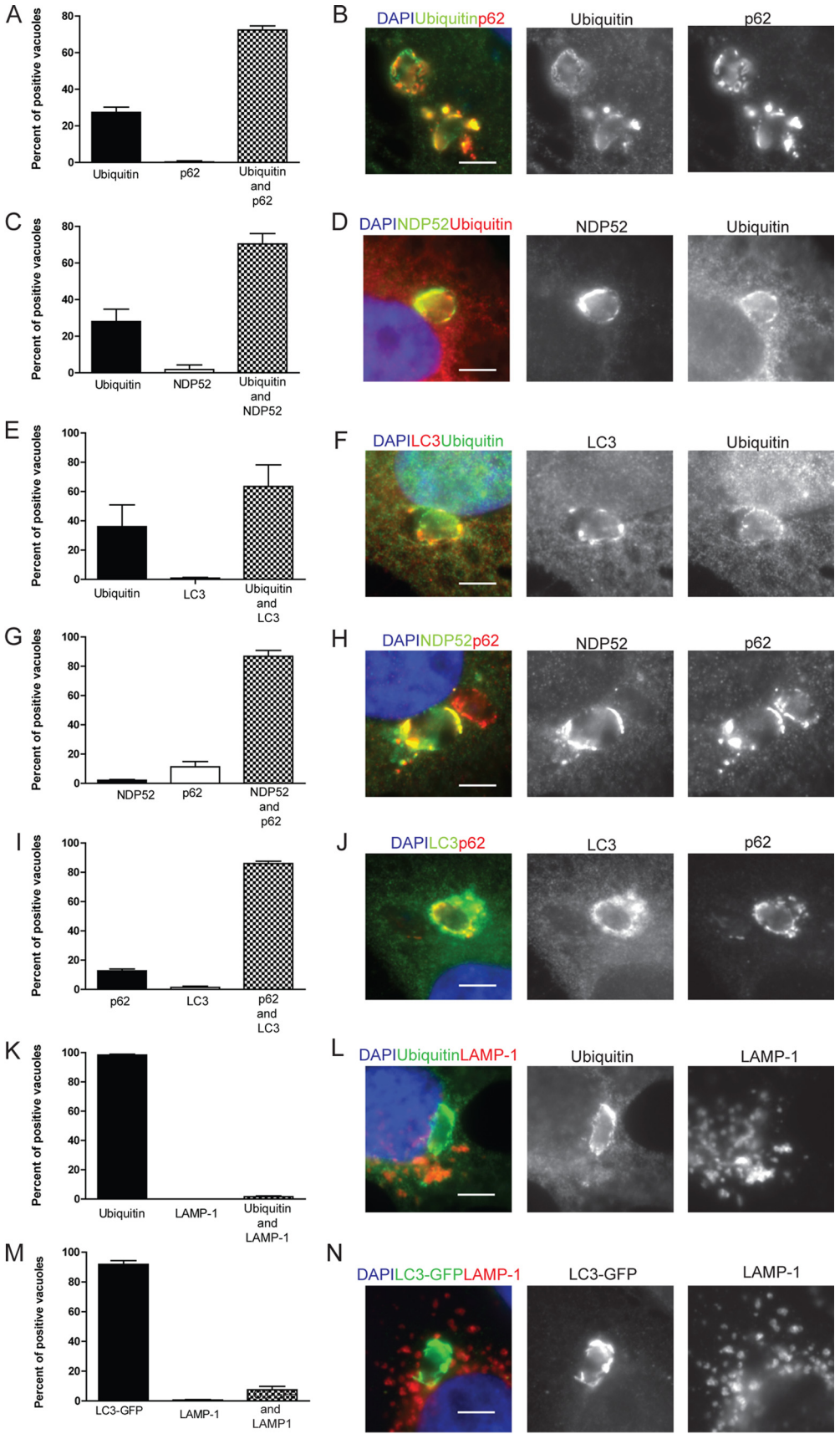
A
Percent of positive vacuoles
Ubiquitin
p62
Ubiquitin and p62
B
DAPIUbiquitinp62
Ubiquitin
p62
C
Percent of positive vacuoles
Ubiquitin
NDP52
Ubiquitin and NDP52
D
DAPINDP52Ubiquitin
NDP52
Ubiquitin
E
Percent of positive vacuoles
Ubiquitin
LC3
Ubiquitin and LC3
F
DAPILC3Ubiquitin
LC3
Ubiquitin
G
Percent of positive vacuoles
NDP52
p62
NDP52 and p62
H
DAPINDP52p62
NDP52
p62
I
Percent of positive vacuoles
p62
LC3
p62 and LC3
J
DAPILC3p62
LC3
p62
K
Percent of positive vacuoles
Ubiquitin
LAMP-1
Ubiquitin and LAMP-1
L
DAPIUbiquitinLAMP-1
Ubiquitin
LAMP-1
M
Percent of positive vacuoles
LC3-GFP
LAMP-1
and LAMP1
N
DAPILC3-GFPLAMP-1
LC3-GFP
LAMP-1

these data suggest that the targeting of PVs by ubiquitin or other adaptors in the autophagy pathway restricts the replication of all strains of parasites in IFN-γ-activated human cells. Thus, the major strain-dependent difference is the much higher level of ubiquitination and recruitment of autophagy adaptors to vacuoles containing type 2 and 3 strain parasites, while type 1 parasites avoid this fate.

Autophagy pathway KO human cells are not able to restrict replication of ubiquitin-positive PVs. To examine the role of autophagy in the growth restriction of *T. gondii* in IFN-γ-activated cells, we examined parasite growth in cells lacking ATG16L1, a critical component of the elongation complex (28). In an experiment similar to that described above, we measured the replication of parasites in ubiquitin-positive PVs in wild-type, ATG16L1 knockout (KO), and complemented cells. Wild-type HeLa cells that were activated with IFN-γ strongly restricted replication in ubiquitin-positive PVs, with 92.7% of the vacuoles containing one or two parasites (Fig. 6A and B). However, in ATG16L1 KO HeLa cells, ubiquitin-positive PVs replicated to significantly higher numbers, similar to the level of replication seen in ubiquitin-negative PVs, with 66.3% of the PVs containing four or more parasites per vacuole (Fig. 6A and B). Stunting of LC3-positive PVs was also reversed in ATG16L1 KO HeLa cells (see Fig. S6A in the supplemental material), as was the wrapping of parasites in multiple membranes, as detected by EM (see Fig. S6B). Complementation of ATG16L1 expression in the KO cell line restored the growth restriction of ubiquitin-positive PVs (Fig. 6A). To extend this analysis, we also examined replication in IFN-γ-activated cells lacking ATG7, which is involved in the lipidation of LC3 (28). ATG7 KO cells were also unable to restrict the growth of ubiquitin-positive PVs in IFN-γ-activated HeLa cells (Fig. 6C and D), while parental wild-type HeLa cells restricted parasite replication (Fig. 6C and D). ATG7 KO clone 1A6 showed a significant defect in the control of the replication of ubiquitin-positive PVs, with more than half of the positive PVs able to replicate to four or more parasites per vacuole. A second ATG7 KO clone, 1A11, showed a more modest phenotype, but ubiquitin-positive PVs were again able to replicate to a significantly higher number than in wild-type cells (Fig. 6C).

To examine whether the upstream activation steps of autophagy are required for the recruitment of ubiquitin to PVs, we depleted U2OS cells of Beclin 1 and ATG14 by using tetracycline-inducible short hairpin RNA (shRNA). In cells depleted of either Beclin 1 or ATG14 (Fig. 6F), ubiquitination of susceptible parasites was not decreased at 6 h postinfection (Fig. 6E). Additionally, we activated autophagy in HeLa cells by using a Tat-Beclin 1 peptide or a control Tat-scrambled peptide. Under these conditions, ubiquitination was not increased in naive cells treated with the Tat-Beclin 1 peptide, despite an increase in LC3-GFP puncta (Fig. 6G and H). Additionally, treatment with the Tat-Beclin 1 peptide did not alter the percentage of ubiquitination of susceptible PVs in IFN-γ-activated cells (Fig. 6G).

DISCUSSION

Although prior studies have shown that IFN-γ activation of human cells restricts the intracellular growth of *T. gondii*, the potential roles of autophagy and xenophagy in this process were unclear. Here we show that *T. gondii* parasites are targeted by a noncanonical autophagy pathway in IFN-γ-activated human cells to restrict growth in a parasite strain-specific manner. Ubiquitin, the autophagy adaptors p62 and NDP52, and LC3 are recruited to high levels around PVs containing susceptible strains of *T. gondii*. LC3-positive PVs were enveloped by multiple membranes that resemble the autophagosomes surrounding group A *Streptococcus* (36). However, *T. gondii*-containing PVs that are targeted by autophagy adapters do not fuse with LAMP-1, and thus, they do not intersect the late endosome or lysosome compartment, as is seen with other pathogens targeted by xenophagy (27, 35). The growth of parasites within membrane-encapsulated PVs was stunted, and replication was rescued by KO of ATG16L1 or ATG7, a protein required for elongation of the autophagosome membrane. Collectively, these findings reveal that a noncanonical autophagy pathway targets *T. gondii* parasites in a strain-specific manner in IFN-γ-activated human cells.

Our findings define a new mechanism for IFN-γ-dependent control of *T. gondii* in human cells that depends on the ubiquitination and recruitment of a set of proteins involved in the autophagy pathway, including p62, NDP52, and LC3. These proteins were recruited in a strain-dependent manner to the PVs of type 2 and 3 parasites, while type 1 parasites largely resisted this recruitment. Importantly, parasite growth was stunted in all ubiquitin-positive vacuoles, regardless of the strain type; thus, the major difference in type 1 strains is their ability to avoid ubiquitination and recruitment of autophagy adaptors. The recruitment of the autophagy proteins was dependent on prior stimulation with IFN-γ, which may be due to the requirement for an IFN-induced protein or to a general upregulation of autophagy adaptors by IFN-γ or through the p38 mitogen-activated protein kinase pathway (40, 41). Ubiquitination and recruitment of autophagy adaptors did not require GBPs, consistent with the lack of a demonstrable role for these proteins in the control of *T. gondii* in IFN-γ-activated human cells (22). Additionally, previously described mouse virulence factors ROP5, ROP18, and ROP17 did not contribute to the strain-dependent differences in the recruitment of autophagy proteins in human cells. Recruitment of autophagy adaptors and LC3 led to parasite growth inhibition, and this was dependent on autophagy proteins ATG16 and ATG7. Since ATG5, ATG12, and ATG16 contribute to a tripartite complex needed for phagophore elongation (28), it is likely that all three proteins are essential to this process, similar to the situation

FIG 2 Colocalization of autophagy adaptors in intracellular *T. gondii*. (A, C, E, G, I, K, M) Quantification of colocalization of host cell markers. The percentage of the subset of type 3 (VEG) PVs that were positive for either a single host cell marker or both was determined by microscopic examination in HeLa cells or in HeLa cells expressing LC3-GFP (M) activated with 5 ng/ml IFN-γ. At 6 h postinfection, cells were fixed and stained for immunofluorescence localization of host cell markers as described below. Each value is the mean ± SEM of three experiments. (K) Mean values ± SD of two experiments with three internal replicates each. (B, D, F, H, J, L, N) Representative images of colocalization of autophagy adaptors surrounding *T. gondii*. Ubiquitin was localized with mouse MAb FK2, p62 was localized with a guinea pig polyclonal antibody, NDP52 was localized with a rabbit polyclonal antibody, LC3 was localized with a rabbit polyclonal antibody, LAMP-1 was localized with a rabbit polyclonal antibody, and GFP-LC3 was localized with mouse MAb 3E6 to GFP, followed by secondary antibodies conjugated with either Alexa Fluor 488 (green) or 594 (red), as indicated. Nuclei were stained with DAPI. Scale bars, 5 μm. See also Fig. S2 in the supplemental material.

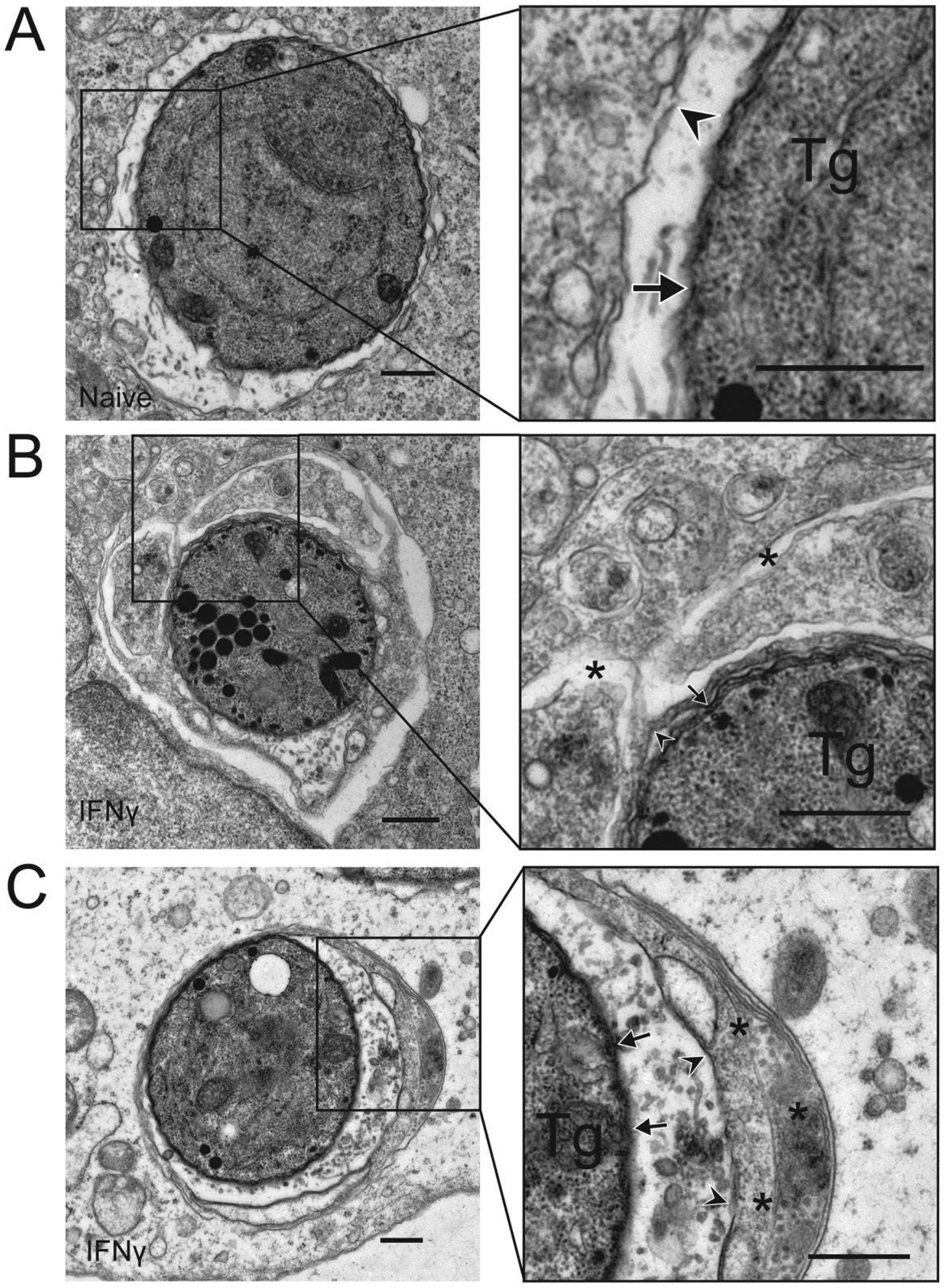

FIG 3 Engulfment of *T. gondii* (Tg) by multiple membranes in IFN-γ-activated cells. (A) Transmission EM reveals the normal architecture of the PVM of a type 3 (VEG) parasite in a naive HeLa cell at 6 h postinfection. (B, C) Additional membranes surround the PVM of a type 3 (VEG) parasite in HeLa cells activated with 5 ng/ml IFN-γ at 6 h postinfection. The arrows indicate the parasite membrane, the arrowheads indicate the PVM, and the asterisks indicate additional membranes. Scale bars, 500 nm. See also Fig. S3 in the supplemental material.

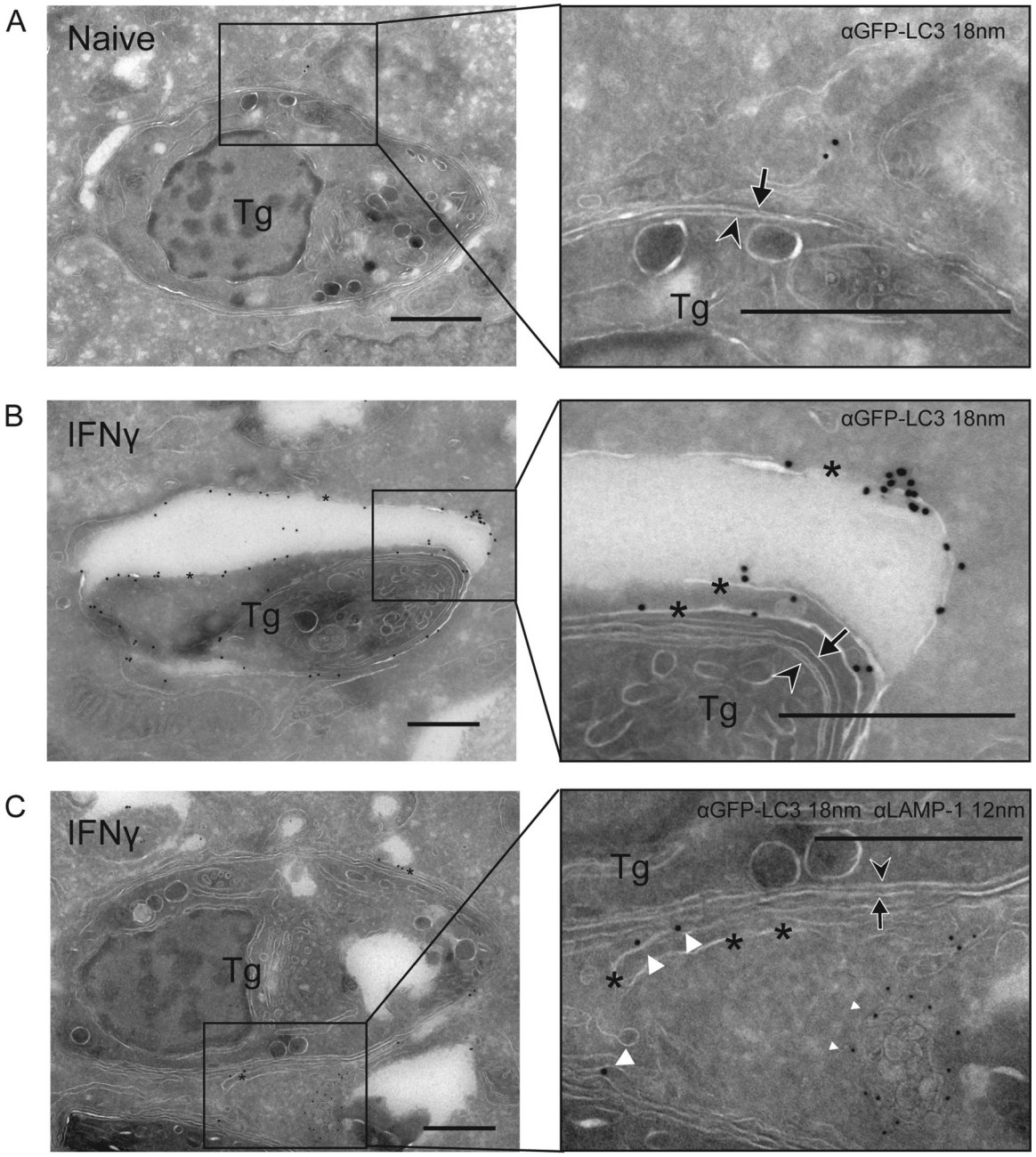

FIG 4 LC3 and LAMP-1 localization in cells infected with *T. gondii* (Tg). Cryo-immuno-EM localization of GFP-LC3 and LAMP-1 in naive (A) or IFN-γ (5 ng/ml)-activated (B, C) HeLa cells infected with type 3 (VEG) parasites at 6 h postinfection. (A, B) GFP-LC3 was localized with a rabbit polyclonal antibody to GFP, followed by goat anti-rabbit IgG conjugated to 18-nm gold. (C) LAMP-1 was localized with rabbit MAb D2D11, followed by donkey anti-rabbit IgG conjugated to 12-nm gold (small white arrowheads), GFP-LC3 was localized with a goat polyclonal antibody to GFP, followed by donkey anti-goat IgG conjugated to 18-nm gold (large white arrowheads). Arrowheads indicate parasite membranes, arrows indicate the PVM, and asterisks indicate additional membranes. Scale bars, 500 nm. See also Fig. S4 in the supplemental material.

in mice (29). In mouse cells activated with IFN-γ, upstream mediators of the autophagy pathway, including Atg14L, Ulk1, and Ulk2, are not required for control of *T. gondii* (29). Here we demonstrate that in human cells depletion of two upstream mediators of autophagy, Beclin 1 and ATG14, does not alter the recruitment of ubiquitin to susceptible strains of *T. gondii* and that induction of autophagy with a peptide derived from Beclin 1 was not sufficient to trigger the recruitment of LC3 to *T. gondii* PVs. Collectively, these data indicate that the autophagy elongation complex is required for growth restriction of *T. gondii* in PVs targeted by ubiquitin. In contrast, upstream components of the autophagy pathway are unlikely to be involved, indicating that these processes do not rely on classical autophagy.

In contrast to our findings, previous studies have failed to find a major role for ATG proteins in the IFN-γ-mediated control of *T. gondii* in human cells. One such study reported normal control

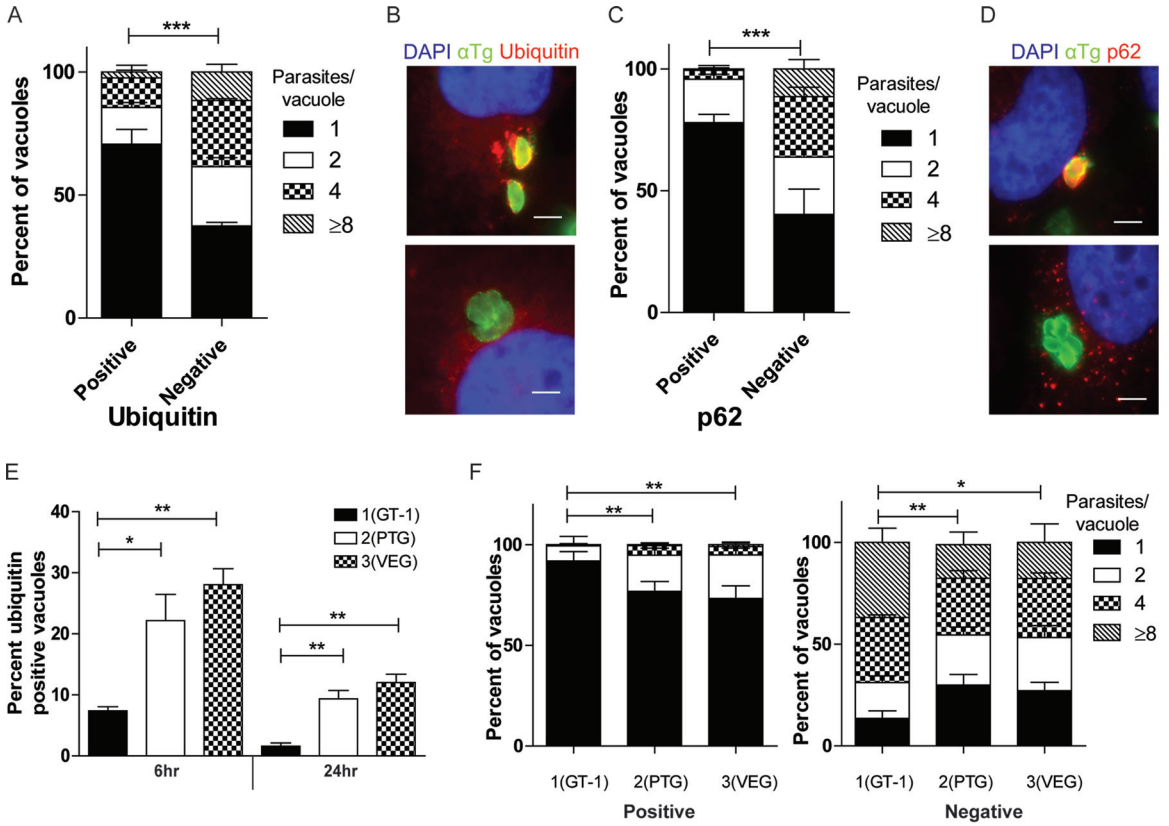

FIG 5 Impaired replication of *T. gondii* in vacuoles targeted by autophagy adaptors. Quantification of parasite replication in vacuoles positive for ubiquitin (A) or p62 (C). The number of parasites per vacuole was assessed by immunostaining for parasite surface or host cell markers, followed by epifluorescence microscopy for type 3 (VEG) parasites in IFN-γ-activated HeLa cells at 24 h postinfection. Each value is the mean ± SEM of three experiments (***, $P < 0.001$; two-way ANOVA). (B, D) Representative immunofluorescence images of vacuoles positive or negative for ubiquitin or p62. (B) Ubiquitin was localized with mouse MAb FK2, followed by goat-anti mouse IgG conjugated to Alexa Fluor 594 (red). Parasites were localized with a rabbit polyclonal antibody to tachyzoites, followed by goat anti-rabbit IgG conjugated to Alexa Fluor 488 (green). (D) p62 was localized with a guinea pig polyclonal antibody, followed by anti-guinea pig IgG conjugated to Alexa Fluor 594 (red). *T. gondii* (αTg) was localized with MAb DG52 to SAG1, followed by goat anti-mouse IgG conjugated to Alexa Fluor 488 (green). Nuclei were stained with DAPI. Scale bars, 5 μm. (E) Quantification of recruitment of ubiquitin to type 1 (GT-1), 2 (PTG), and 3 (VEG) parasites at 6 or 24 h postinfection in IFN-γ-activated HeLa cells. Each value is the mean ± SEM of three experiments (**, $P < 0.01$; *, $P < 0.05$; one-way ANOVA). Strains were compared to each other at the same time point. (F) Quantification of parasite replication of type 1 (GT-1), 2 (PTG), and 3 (VEG) parasites in vacuoles positive or negative for ubiquitin at 24 h postinfection in IFN-γ-activated HeLa cells. Replication was quantified as described above. The total numbers of positive vacuoles counted for replication were as follows: type 1, 90; type 2, 450; type 3, 450 (**, $P < 0.01$; *, $P < 0.05$; two-way ANOVA). See also Fig. S5 in the supplemental material.

of *T. gondii* replication in IFN-γ-activated human cells depleted of ATG5; however, this result may have been due to the use of a type 1 strain (24), which we have shown is resistant to this pathway, or incomplete knockdown by small interfering RNA. Another study failed to observe a role for ATG16L1 in the control of a type 2 strain of *T. gondii* in IFN-γ-activated human cells, as detected by a parasite luciferase-based growth assay (22). Our ability to discern a role for ATG proteins in IFN-γ-treated human cells may be due to our use of a more sensitive assay that distinguishes the fate of individual parasite-containing vacuoles. By examining individual vacuoles, we demonstrate that type 1 strain parasites largely avoid the recruitment of ubiquitin and autophagy adaptors and that therefore their replication is unimpeded. In contrast, a large fraction (i.e., 20 to 30%) of vacuoles containing type 2 and 3 parasites recruit these adaptors and are stunted in growth. Although susceptible type 2 and 3 strains recruit LC3 to a portion of the PVs, not all parasites are affected by this growth-restricting pathway. Thus, incomplete targeting may explain why the role of ATG proteins was not evident in assays that monitored total population growth. The reasons for the observed heterogeneity in the targeting of susceptible PVs are unclear, but similar finding have been reported for bacterial pathogens that are targeted by xenophagy (42). Collectively, these findings indicate that recruitment of autophagy adaptors leads to strain-specific restriction of *T. gondii* growth, although other host factors also contribute to the control of parasite replication in IFN-γ-activated human cells.

Despite the findings that the same core set of Atg proteins is essential in mouse and human cells, the pathways they control are quite different. In mouse cells, Atg3, Atg7, and a complex consisting of Atg5, Atg12, and Atg16 are required for the recruitment of IRGs and GBPs, which results in vesiculation of the PVM and destruction of the parasite (22, 29, 30). In contrast, the present study shows that in human cells, ATG16L1 and ATG7 are required for a process that results in wrapping of the PV in multiple host membranes. Membrane envelopment in human cells did not led to vacuole destruction or delivery to lysosomes but rather restricted growth. The PV surrounding *T. gondii* is normally porous to small molecules (43), suggesting that this may be an important

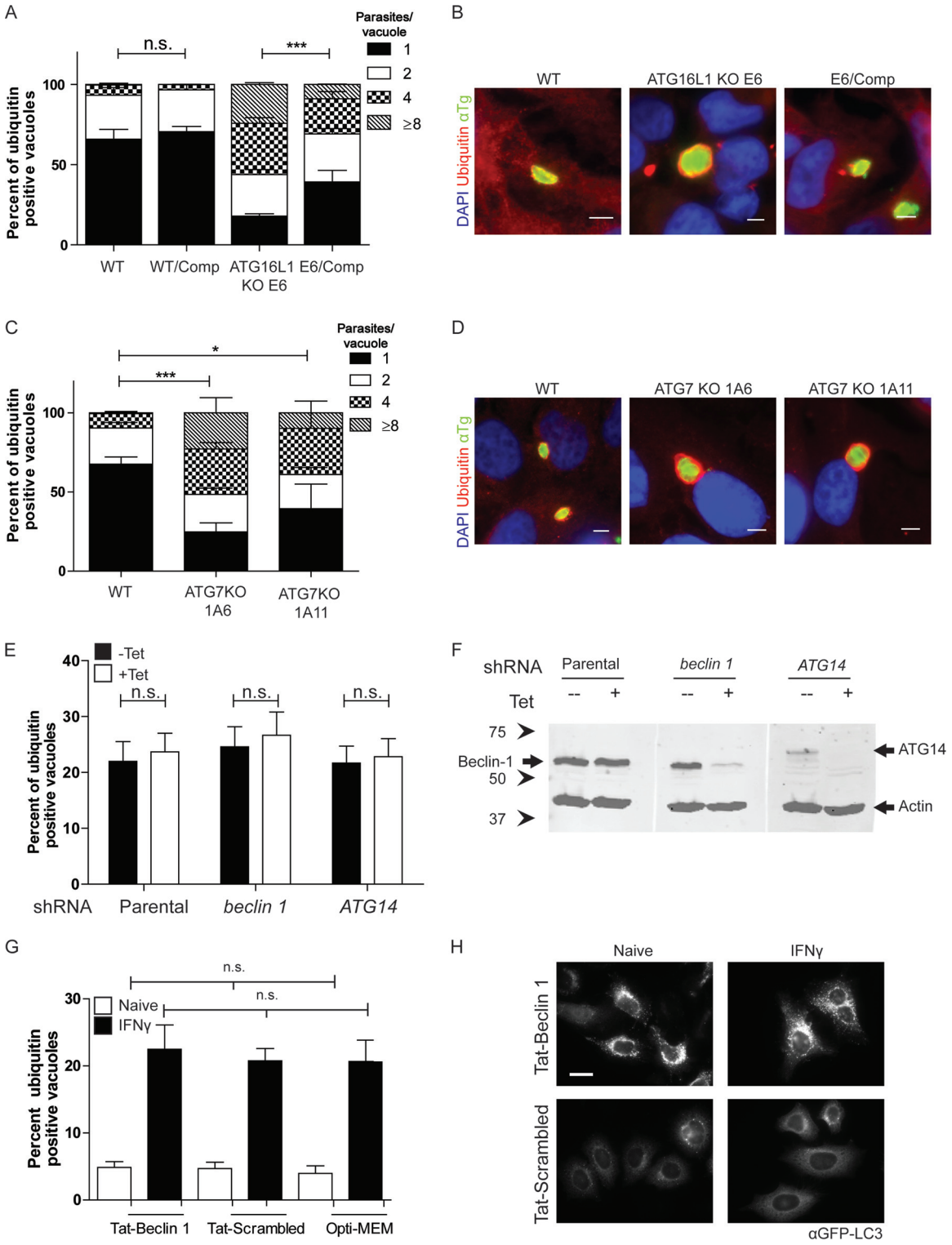

FIG 6 Replication of *T. gondii* in autophagy-deficient HeLa cells. (A) Replication of type 3 (VEG) *T. gondii* in vacuoles positive for ubiquitin in IFN-γ-activated wild-type (WT), ATG16L1 KO (clone E6), or ATG16L1-complemented (WT/Comp or E6/comp) host cell strains at 24 h postinfection. Each value is the mean ± SEM of three experiments (***, $P < 0.001$; two-way ANOVA). (B) Representative fluorescence images of *T. gondii* vacuoles in ATG16L1 KO or complemented strains. Ubiquitin was localized with mouse MAb FK2, followed by goat anti-mouse IgG conjugated to Alexa Fluor 594 (red). Parasites were localized with a rabbit polyclonal antibody to tachyzoites (αTg), followed by goat anti-rabbit IgG conjugated to Alexa Fluor 488 (green). Scale bars, 5 μm. (C) Replication of type 3 (VEG) *T. gondii* positive for ubiquitin in IFN-γ-activated ATG7 KO HeLa cells at 24 h postinfection. Each value is the mean ± SEM of three experiments (***, $P < 0.001$; two-way ANOVA). (D) Representative images of *T. gondii* vacuoles in wild-type (WT) HeLa cells or ATG7 KO clones (1A6 or 1A11). Ubiquitin was localized with mouse MAb FK2, followed by goat anti-mouse IgG conjugated to Alexa Fluor 594 (red). Parasites were localized with a rabbit polyclonal antibody to tachyzoites (αTg), followed by goat anti-rabbit IgG conjugated to Alexa Fluor 488 (green). Scale bars, 5 μm. (E) Quantification of recruitment of ubiquitin to

(Continued)

route for nutrient uptake from the cytosol. Therefore, the envelopment of the PV in multiple membranes may impair the acquisition of essential nutrients or lipids. Consistent with this, deletion of ATG16L1 or ATG7 led to loss of membrane envelopment and reversal of growth inhibition in IFN-γ-activated HeLa cells. Although human cells can control *T. gondii* in response to IFN-γ by induction of IDO and the depletion of host cell tryptophan (23), tryptophan supplementation did not rescue the growth repression associated with ubiquitin recruitment. Additionally, although we did observe a low level of cell death and *T. gondii* egress upon the activation of human cells with IFN-γ, this outcome was not strain dependent and is unlikely to account for the findings presented here. Instead, our findings reveal a novel pathway of ATG-dependent membrane recruitment that leads to inhibition of parasite replication.

The recognition of bacteria by autophagy has been associated with a reduction in the burden of infectious organisms because of the fusion of the autophagosome with lysosomes and subsequent killing of the bacteria (35). Although some bacteria, such as *Mycobacterium tuberculosis*, *Chlamydia trachomatis*, and adherent invasive *Escherichia coli*, are able to manipulate this pathway to reduce their fusion with and/or acidification of lysosomes (35, 44–47), they have all been reported to acquire LAMP-1 on the autophagosome to a substantial degree (48). Similarly, activation of CD40 on mouse and human cells leads to recruitment of autophagy adaptors and delivery of *T. gondii* to lysosomes, where they are destroyed by a process that is independent of IFN-γ (25–27). In contrast, we demonstrate that, in human cells, LAMP-1 does not accumulate on PVs targeted by autophagy, nor are susceptible parasites cleared from IFN-γ-activated HeLa cells. This result suggests that susceptible PVs targeted by LC3 do not fuse with either late endosome or lysosomes, since both host compartments are enriched in this membrane marker (49). It has been shown that *T. gondii* parasites actively invade host cells and establish a PV that does not intersect the endocytic pathway, fuse with endosomes or lysosomes, or become acidified (8, 10–12). Two models have been proposed to explain how *T. gondii* avoids fusion with the host endomembrane system: (i) an active block in endocytic fusion and (ii) absence of fusion-promoting signals on the PVM (9). Our data suggest that prevention by the parasite of LAMP-1 accumulation on the PV is an active process, since PVs that are targeted by ubiquitin, autophagy adaptors, and LC3 still do not fuse with endosomes or lysosomes. In this regard, the presence of *T. gondii* PVs enveloped by multiple membranes may represent a process of targeting for autophagosome engulfment in the absence of delivery to lysosomes.

Here we define a new pathway for cell-autonomous immune control of *T. gondii* in IFN-γ-activated human cells. The recruitment of autophagy proteins and stunting of targeted PVs occur in a strain-specific manner, suggesting that there are novel virulence factors that target this mechanism of cell-autonomous immunity in human cells. Understanding the mechanisms by which parasites are able to thwart human innate immune defenses may influence the design of novel therapeutics to treat toxoplasmosis.

MATERIALS AND METHODS

(For additional materials and methods used in this study, see Text S1 in the supplemental material.)

Parasite strains and culture. Type 1 (GT-1:ATCC 50853), 2 (PTG: ATCC 50841), and 3 (VEG) (4) parasite strains were cultured in human foreskin fibroblasts (HFFs) grown in Dulbecco's modified Eagle's medium (DMEM) supplemented with 10% fetal bovine serum (FBS; HyClone), 2 mM glutamine (Sigma), 10 mM HEPES (pH 7.5; Sigma), and 20 μg/ml gentamicin at 37°C in 5% CO_2. For all parasite infections, parasites were allowed to egress naturally and were harvested as described previously (50). All strains and host cell lines were determined to be mycoplasma negative with the e-Myco plus kit (Intron Biotechnology).

Cell culture. HeLa cells were grown in minimum essential medium (Sigma) supplemented with 10% defined FBS (HyClone), 4 mM glutamine, and 10 mM HEPES, pH 7.5. HeLa cells stably expressing LC3-GFP were grown in the above medium supplemented with 100 μg/ml G418 (Sigma). ATG16L1 and ATG7 KO HeLa cells were grown in DMEM (Gibco) supplemented with 10% defined FBS (HyClone), 4 mM glutamine, and 10 mM HEPES, pH 7.5 (Sigma). U2OS^{TetR}, U2OS^{TetR}/*shATG14*, and U2OS^{TetR}/*shbeclin 1* cells were cultured in Iscove's modified Dulbecco's medium (Gibco) supplemented with 10% defined, tetracycline-free FBS (HyClone), 4 mM glutamine, and 10 mM HEPES, pH 7.5.

Autophagy-deficient cell lines. ATG16L1-deficient HeLa cells were generated with the px330 plasmid CRISPR system as described previously (51). HeLa cells were transfected with the Cas9 vector containing *ATG16L1*-specific subgenomic RNA (sgRNA) sequences located in exon 2 of *ATG16L1* isoform 1 by using FuGENE (Roche) according to the manufacturer's instructions. At 48 h posttransfection, cells were plated in limiting dilution in 96-well plates to isolate single cell clones. To confirm complete *ATG16L1* KO, DNA was extracted with DNeasy (Qiagen) and *ATG16L1* exon 2 was PCR amplified and sequenced to identify clones with frameshift mutations in all loci. ATG7 HeLa cells were obtained from the Genome Engineering and iPSC Center at the Washington University School of Medicine. HeLa cells were transfected with the Cas9 vector containing *ATG7*-specific sgRNA sequences located in exon 3 of *ATG7*. Cells were plated in limiting dilution in 96-well plates to isolate single cell clones. To confirm complete *ATG16L1* KO, DNA was extracted and *ATG7* exon 3 was PCR amplified and sequenced to identify clones with frameshift mutations. To generate the ATG16L1 rescue line, *ATG16L1* cDNA was inserted into a modified CSGW lentiviral vector and cotransfected into HEK293T cells with a vesicular stomatitis virus G protein expression plasmid and a gag-pol expression plasmid. After 48 h, medium containing lentivirus was harvested and used to infect *ATG16L1* KO HeLa cells. After 48 h, 3 μg/ml blasticidin was added to select for cells with a stably inte-

Figure Legend Continued

type 3 (VEG) parasites in IFN-γ-activated (5 ng/ml) U2OS cells treated with tetracycline-inducible shRNA in the presence or absence of tetracycline at 6 h postinfection. Each value is the mean ± SEM of three experiments (n.s., not significant; two-way ANOVA). (F) Expression of Beclin 1 and ATG14 detected by Western blotting of lysates from parental U2OS cells or ± tetracycline-induced shRNA knockdown of Beclin 1 and ATG14. Beclin 1 and ATG14 were detected with a rabbit MAb (Beclin 1) or a rabbit polyclonal antibody (ATG14), followed by LiCor IRDye 800CW goat anti-rabbit IgG (green). Actin was used as a loading control and detected with mouse MAb C4, followed by LiCor IRDye 680CW goat anti-mouse IgG (red). Arrowheads indicate Beclin 1 or ATG14 protein. The values to the left are molecular sizes in kilodaltons. (G) Quantification of recruitment of ubiquitin to type 3 (VEG) parasites in naive or IFN-γ-activated HeLa cells treated with 25 μM Tat-Beclin 1, Tat-scrambled peptide, or Opti-MEM at 6 h postinfection. Each value is the mean ± SD of two experiments with three internal replicates and a total of six coverslips. n.s., not significant; Kruskal-Wallis test. (H) Representative fluorescence images of HeLa cells expressing LC3-GFP treated with 25 μM Tat-Beclin 1 or Tat-scrambled peptide for 3 h. GFP-LC3 was localized with mouse MAb 3E6 against GFP, followed by goat anti-mouse IgG conjugated to Alexa Fluor 488. Scale bar, 20 nm. See also Fig. S6 in the supplemental material.

grated ATG16L1-expressing provirus. U2OS^{TetR}, U2OS^{TetR}/*shATG14*, and U2OS^{TetR}/*shbeclin 1* cells were generated as previously described (52).

Western blot analysis. U2OS cells for Western blot analysis were lysed in 1% NP-40 lysis buffer (1% NP-40, 150 mM NaCl, 25 mM Tris, 1 mM EDTA, pH 7.4) with protease inhibitors. Samples were resuspended in denaturing SDS sample buffer, resolved on a 10% acrylamide gel, and transferred to a nitrocellulose membrane. Blots were probed with rabbit monoclonal antibody (MAb) D40C5 to Beclin 1 (Cell Signaling), rabbit anti-ATG14 antibody (Cell Signaling), or MAb C4 against actin (Millipore), followed by goat anti-rabbit or -mouse IgG conjugated to IRDye 680 or 800, as indicated (LI-COR).

Antibodies. The *T. gondii* PVM was localized with mouse MAb tg17-113 against GRA5 (53) or rabbit polyclonal serum to GRA7 (54). Intracellular *T. gondii* parasites were localized with either mouse MAb DG52 against SAG1 or rabbit polyclonal serum to type 1 (RH) strain tachyzoites (this serum cross-reacts with all of the *T. gondii* strains used here). Ubiquitin was localized with mouse MAb FK2 (EMD Millipore). p62 was localized with a guinea pig polyclonal antibody specific to the C terminus (Progen). NDP52 was localized with a rabbit polyclonal antibody (Proteintech). LC3 was localized with a rabbit polyclonal antibody (MBL). LAMP-1 was localized with rabbit MAb D2D11 (Cell Signaling). GFP was localized with a rabbit polyclonal antibody (Abcam) or mouse MAb 3E6 (Life Technologies). Actin was localized with mouse MAb C4 (Invitrogen). Secondary antibodies conjugated to Alexa Fluor 488 or 594 (Invitrogen) were used for detection by immunofluorescence.

Autophagy induction. Tat-Beclin 1 and Tat-scrambled peptides (AnaSpec Inc.) were resuspended in sterile H_2O and stored at −80°C. Peptides were resuspended to 25 μM in Opti-MEM (Gibco) acidified to pH 7 with HCl. Cells were washed with PBS, and peptides were added to cells at 3 h preinfection.

Beclin 1 and ATG14 knockdown. Tetracycline-inducible shRNA-treated U2OS cells were cultured in the presence of 1 μg/ml anhydrotetracyline (Clontech) for 5 days. Cells were then seeded onto glass coverslips, allowed to adhere in the presence of anhydrotetracyline overnight, and then activated with a final IFN-γ concentration of 5 ng/ml for 24 h prior to infection. Cells for Western blot analysis were harvested at the same time as fixation for *T. gondii*-infected cells.

Immunofluorescence assays. Cell monolayers were fixed in 4% formaldehyde, permeabilized with 0.05% saponin, and stained with primary and secondary antibodies as described previously (55). Samples were visualized with a Zeiss Axioskop 2 MOT Plus microscope equipped for epifluorescence and with a 63× Plan-Apochromat lens, numerical aperture 1.40 (Carl Zeiss, Inc., Thornwood, NY). Images were acquired with an AxioCam MRm camera (Carl Zeiss, Inc.) with AxioVision v4.6 and processed with similar linear adjustments for all samples in Photoshop CS4 v9.

Fluorescence quantification of positive vacuoles. To determine the mean fluorescence of each host marker on the parasite vacuole, HeLa cells were activated with 5 ng/ml IFN-γ for 24 h, infected with parasites for 2 h, washed three times with PBS, and recultured with complete medium. Cells were fixed at 6 h postinfection, and parasites and host cell markers were localized with antibodies as described previously. On each of three coverslips, five random fields were captured for a total of 15 images under each condition. This was repeated for three separate experiments for a total of 45 images analyzed under each condition. With the Velocity software (Velocity Software Inc.), a region of interest (ROI) was drawn over the *T. gondii* vacuole and the mean red fluorescence in this area was obtained. Three background ROIs, two in infected cells and one in a noninfected cell, were also obtained. These three background values were averaged and subtracted from the mean fluorescence intensity of each ROI. The data shown are for each ROI with the background subtracted, and all negative values were set to zero.

Visual assessment of positive vacuoles. To examine the distribution of host markers, samples were fixed at 6 h postinfection in HeLa cells activated as described above. After staining with appropriate primary and secondary antibodies, recruitment was determined by first visualizing the parasitophorous vacuole or parasite marker and then assessing whether there was an accumulation of host protein around each parasite. The percentage of positive parasites was determined from at least 100 parasites per coverslip.

Intracellular replication assays. To examine intracellular replication of *T. gondii*, IFN-γ-activated HeLa cells were infected with parasites for 2 h, washed three times with PBS, and fed with fresh medium. Cells were fixed at 24 h postinfection, and intracellular parasites were localized with MAb DG52 or a rabbit polyclonal antibody to RH strain tachyzoites. Secondary antibodies recognizing the species of primary antibody conjugated to Alexa Fluor 488 or 594 were used as indicated. The number of parasites per vacuole was determined by manual counting on a fluorescence microscope. The number of parasites per vacuole was determined from at least 50 vacuoles on three individual coverslips.

Transmission EM. HeLa cells were activated with 5 ng/ml IFN-γ for 24 h prior to infection. Where indicated, cells were infected with freshly egressed parasites for 2 h, washed three times with PBS, and then fixed at 6 h postinfection. For ultrastructural analysis, cells were fixed in 2% paraformaldehyde--2.5% glutaraldehyde (Polysciences) in 100 mM phosphate buffer (pH 7.2) for 1 h at room temperature, processed, and examined as described previously (30, 32). For immuno-EM, HeLa cells stably expressing GFP were fixed in 4% paraformaldehyde--0.05% glutaraldehyde (Polysciences) in 100 mM piperazine-*N*,*N*[prime]-bis(2-ethanesulfonic acid) (PIPES)--0.5 mM $MgCl_2$ (pH 7.2) for 1 h at 4°C and processed as described previously (32). Sections were stained with rabbit polyclonal antibody to GFP (Abnova), goat polyclonal antibody to GFP (Abcam), or rabbit MAb D2D11 against LAMP-1 (Cell Signaling), followed by gold-conjugated secondary antibodies (Jackson ImmunoResearch Laboratories). Sections were stained and viewed with a JEOL 1200EX transmission electron microscope (JEOL USA) as described previously (32). Parallel controls with the primary antibodies omitted were consistently negative at the concentration of colloidal-gold-conjugated secondary antibodies used in these studies.

Statistics. Statistical analyses were conducted with PRISM (GraphPad). Results were compared with the Kruskal-Wallis test or one- or two-way analysis of variance (ANOVA), as noted. *P* values of $\leq$0.05 were considered significant. Data were graphed as the mean ± the standard error of the mean (SEM) or the standard deviation (SD), as indicated in the figure legends.

SUPPLEMENTAL MATERIAL

Supplemental material for this article may be found at http://mbio.asm.org/lookup/suppl/doi:10.1128/mBio.01157-15/-/DCSupplemental.

Text S1, PDF file, 0.1 MB.
Figure S1, PDF file, 0.2 MB.
Figure S2, PDF file, 0.3 MB.
Figure S3, PDF file, 0.5 MB.
Figure S4, PDF file, 0.3 MB.
Figure S5, PDF file, 0.2 MB.
Figure S6, PDF file, 0.5 MB.

ACKNOWLEDGMENTS

We thank the Genome Engineering Center at Washington University School of Medicine for ATG7 KO cells, Jennifer Barks for technical assistance, and the members of the Sibley Lab for helpful discussions.

This study was supported by grants from the NIH (AI118426, AI036629, U19 AI109725).

E.M.S. designed and performed the majority of the experiments, analyzed the data, generated the figures, and contributed to the writing of the manuscript. R.C.O. provided assistance with ATG16L1 complementation and ATG7 KO cells. K.G.L. and R.J.X. provided ATG16L1 KO cells and helpful discussions. W.L.B. performed the EM experiments, H.W.V. and B.L. provided key reagents and insight into the autophagy pathway. L.D.S. supervised the studies and contributed to the design and analyses of the

experiments and the writing and editing of the manuscript. All of the authors approved the manuscript.

REFERENCES

1. **Dubey JP**. 2010. Toxoplasmosis of animals and humans. CRC Press, Boca Raton, FL.
2. **Pappas G, Roussos N, Falagas ME**. 2009. Toxoplasmosis snapshots: global status of *Toxoplasma gondii* seroprevalence and implications for pregnancy and congenital toxoplasmosis. Int J Parasitol **39:**1385–1394. http://dx.doi.org/10.1016/j.ijpara.2009.04.003.
3. **Sibley LD, Ajioka JW**. 2008. Population structure of *Toxoplasma gondii*: clonal expansion driven by infrequent recombination and selective sweeps. Annu Rev Microbiol **62:**329–351. http://dx.doi.org/10.1146/annurev.micro.62.081307.162925.
4. **Howe DK, Sibley LD**. 1995. *Toxoplasma gondii* comprises three clonal lineages: correlation of parasite genotype with human disease. J Infect Dis **172:**1561–1566. http://dx.doi.org/10.1093/infdis/172.6.1561.
5. **Sibley LD, Khan A, Ajioka JW, Rosenthal BM**. 2009. Genetic diversity of Toxoplasma gondii in animals and humans. Philos Trans R Soc Lond B Biol Sci **364:**2749–2761. http://dx.doi.org/10.1098/rstb.2009.0087.
6. **Suss-Toby E, Zimmerberg J, Ward GE**. 1996. *Toxoplasma* invasion: the parasitophorous vacuole is formed from host cell plasma membrane and pinches off via a fusion pore. Proc Natl Acad Sci U S A **93:**8413–8418. http://dx.doi.org/10.1073/pnas.93.16.8413.
7. **Charron AJ, Sibley LD**. 2004. Molecular partitioning during host cell penetration by *Toxoplasma gondii*. Traffic **5:**855–867. http://dx.doi.org/10.1111/j.1600-0854.2004.00228.x.
8. **Mordue DG, Desai N, Dustin M, Sibley LD**. 1999. Invasion by *Toxoplasma gondii* establishes a moving junction that selectively excludes host cell plasma membrane proteins on the basis of their membrane anchoring. J Exp Med **190:**1783–1792. http://dx.doi.org/10.1084/jem.190.12.1783.
9. **Sibley LD**. 2011. Invasion and intracellular survival by protozoan parasites. Immunol Rev **240:**72–91. http://dx.doi.org/10.1111/j.1600-065X.2010.00990.x.
10. **Jones TC, Hirsch JG**. 1972. The interaction of *Toxoplasma gondii* and mammalian cells. II. The absence of lysosomal fusion with phagocytic vacuoles containing living parasites. J Exp Med **136:**1173–1194. http://dx.doi.org/10.1084/jem.136.5.1173.
11. **Mordue DG, Håkansson S, Niesman I, Sibley LD**. 1999. *Toxoplasma gondii* resides in a vacuole that avoids fusion with host cell endocytic and exocytic vesicular trafficking pathways. Exp Parasitol **92:**87–99. http://dx.doi.org/10.1006/expr.1999.4412.
12. **Sibley LD, Weidner E, Krahenbuhl JL**. 1985. Phagosome acidification blocked by intracellular *Toxoplasma gondii*. Nature **315:**416–419. http://dx.doi.org/10.1038/315416a0.
13. **Howard JC, Hunn JP, Steinfeldt T**. 2011. The IRG protein-based resistance mechanism in mice and its relation to virulence in *Toxoplasma gondii*. Curr Opin Microbiol **14:**414–421. http://dx.doi.org/10.1016/j.mib.2011.07.002.
14. **MacMicking JD**. 2012. Interferon-inducible effector mechanisms in cell-autonomous immunity. Nat Rev Immunol **12:**367–382. http://dx.doi.org/10.1038/nri3210.
15. **Khaminets A, Hunn JP, Könen-Waisman S, Zhao YO, Preukschat D, Coers J, Boyle JP, Ong YC, Boothroyd JC, Reichmann G, Howard JC**. 2010. Coordinated loading of IRG resistance GTPases on to the *Toxoplasma gondii* parasitophorous vacuole. Cell Microbiol **12:**939–961. http://dx.doi.org/10.1111/j.1462-5822.2010.01443.x.
16. **Zhao Y, Ferguson DJ, Wilson DC, Howard JC, Sibley LD, Yap GS**. 2009. Virulent *Toxoplasma gondii* evade immunity-related GTPas-mediated parasite vacuole disruption within primed macrophages. J Immunol **182:**3775–3781. http://dx.doi.org/10.4049/jimmunol.0804190.
17. **Zhao YO, Khaminets A, Hunn JP, Howard JC**. 2009. Disruption of the *Toxoplasma gondii* parasitophorous vacuole by IFN-gamma-inducible immunity-related GTPases (IRG proteins) triggers necrotic cell death. PLoS Pathog **5:**e1000288. http://dx.doi.org/10.1371/journal.ppat.1000288.
18. **Degrandi D, Kravets E, Konermann C, Beuter-Gunia C, Klümpers V, Lahme S, Wischmann E, Mausberg AK, Beer-Hammer S, Pfeffer K**. 2013. Murine guanylate binding protein 2 (mGBP2) controls *Toxoplasma gondii* replication. Proc Natl Acad Sci U S A **110:**294–299. http://dx.doi.org/10.1073/pnas.1205635110.
19. **Selleck EM, Fentress SJ, Beatty WL, Degrandi D, Pfeffer K, Virgin HW, Macmicking JD, Sibley LD**. 2013. Guanylate-binding protein 1 (Gbp1) contributes to cell-autonomous immunity against *Toxoplasma gondii*. PLoS Pathog **9:**e1003320. http://dx.doi.org/10.1371/journal.ppat.1003320.
20. **Yamamoto M, Okuyama M, Ma JS, Kimura T, Kamiyama N, Saiga H, Ohshima J, Sasai M, Kayama H, Okamoto T, Huang DC, Soldati-Favre D, Horie K, Takeda J, Takeda K**. 2012. A cluster of interferon-gamma-inducible p65 GTPases plays a critical role in host defense against *Toxoplasma gondii*. Immunity **37:**302–313. http://dx.doi.org/10.1016/j.immuni.2012.06.009.
21. **Hunter CA, Sibley LD**. 2012. Modulation of innate immunity by *Toxoplasma gondii* virulence effectors. Nat Rev Microbiol **10:**766–778. http://dx.doi.org/10.1038/nrmicro2858.
22. **Ohshima J, Lee Y, Sasai M, Saitoh T, Su Ma JJ, Kamiyama N, Matsuura Y, Pann-Ghill S, Hayashi M, Ebisu S, Takeda K, Akira S, Yamamoto M**. 2014. Role of mouse and human autophagy proteins in IFN-gamma-induced cell-autonomous responses against *Toxoplasma gondii*. J Immunol **192:**3328–3335. http://dx.doi.org/10.4049/jimmunol.1302822.
23. **Pfefferkorn ER**. 1984. Interferon-gamma blocks the growth of *Toxoplasma gondii* in human fibroblasts by inducing the host to degrade tryptophan. Proc Natl Acad Sci U S A **81:**908–912. http://dx.doi.org/10.1073/pnas.81.3.908.
24. **Niedelman W, Sprokholt JK, Clough B, Frickel EM, Saeij JP**. 2013. Cell death of gamma interferon-stimulated human fibroblasts upon *Toxoplasma gondii* infection induces early parasite egress and limits parasite replication. Infect Immun **81:**4341–4349. http://dx.doi.org/10.1128/IAI.00416-13.
25. **Andrade RM, Wessendarp M, Gubbels MJ, Striepen B, Subauste CS**. 2006. CD40 induces macrophage anti-*Toxoplasma gondii* activity by triggering autophagy-dependent fusion of pathogen-containing vacuoles and lysosomes. J Clin Invest **116:**2366–2377. http://dx.doi.org/10.1172/JCI28796.
26. **Subauste CS**. 2009. CD40, autophagy and Toxoplasma gondii. Mem Inst Oswaldo Cruz **104:**267–272. http://dx.doi.org/10.1590/S0074-02762009000200020.
27. **Van Grol J, Muniz-Feliciano L, Portillo JA, Bonilha VL, Subauste CS**. 2013. CD40 induces anti-*Toxoplasma gondii* activity in nonhematopoietic cells dependent on autophagy proteins. Infect Immun **81:**2002–2011. http://dx.doi.org/10.1128/IAI.01145-12.
28. **Levine B, Mizushima N, Virgin HW**. 2011. Autophagy in immunity and inflammation. Nature **469:**323–335. http://dx.doi.org/10.1038/nature09782.
29. **Choi J, Park S, Biering SB, Selleck E, Liu CY, Zhang X, Fujita N, Saitoh T, Akira S, Yoshimori T, Sibley LD, Hwang S, Virgin HW**. 2014. The parasitophorous vacuole membrane of Toxoplasma gondii is targeted for disruption by ubiquitin-like conjugation systems of autophagy. Immunity **40:**924–935. http://dx.doi.org/10.1016/j.immuni.2014.05.006.
30. **Zhao Z, Fux B, Goodwin M, Dunay IR, Strong D, Miller BC, Cadwell K, Delgado MA, Ponpuak M, Green KG, Schmidt RE, Mizushima N, Deretic V, Sibley LD, Virgin HW**. 2008. Autophagosome-independent essential function for the autophagy protein Atg5 in cellular immunity to intracellular pathogens. Cell Host Microbe **4:**458–469. http://dx.doi.org/10.1016/j.chom.2008.10.003.
31. **Traver MK, Henry SC, Cantillana V, Oliver T, Hunn JP, Howard JC, Beer S, Pfeffer K, Coers J, Taylor GA**. 2011. Immunity-related GTPase M (IRGM) proteins influence the localization of guanylate-binding protein 2 (GBP2) by modulating macroautophagy. J Biol Chem **286:**30471–30480. http://dx.doi.org/10.1074/jbc.M111.251967.
32. **Fentress SJ, Behnke MS, Dunay IR, Moashayekhi M, Rommereim LM, Fox BA, Bzik DJ, Tayor GA, Turk BE, Lichti CF, Townsend RR, Qiu W, Hui R, Beatty WL, Sibley LD**. 2010. Phosphorylation of immunity-related GTPases by a parasite secretory kinase promotes macrophage survival and virulence. Cell Host Microbe **16:**484–495.
33. **Deretic V, Saitoh T, Akira S**. 2013. Autophagy in infection, inflammation and immunity. Nat Rev Immunol **13:**722–737. http://dx.doi.org/10.1038/nri3532.
34. **Birmingham CL, Smith AC, Bakowski MA, Yoshimori T, Brumell JH**. 2006. Autophagy controls salmonella infection in response to damage to the salmonella-containing vacuole. J Biol Chem **281:**11374–11383. http://dx.doi.org/10.1074/jbc.M509157200.
35. **Huang J, Brumell JH**. 2014. Bacteria-autophagy interplay: a battle for survival. Nat Rev Microbiol **12:**101–114. http://dx.doi.org/10.1038/nrmicro3160.

36. **Nakagawa I, Amano A, Mizushima N, Yamamoto A, Yamaguchi H, Kamimoto T, Nara A, Funao J, Nakata M, Tsuda K, Hamada S, Yoshimori T.** 2004. Autophagy defends cells against invading group A streptococcus. Science **306:**1037–1040. http://dx.doi.org/10.1126/science.1103966.
37. **Rich KA, Burkett C, Webster P.** 2003. Cytoplasmic bacteria can be targets for autophagy. Cell Microbiol **5:**455–468. http://dx.doi.org/10.1046/j.1462-5822.2003.00292.x.
38. **Starr T, Child R, Wehrly TD, Hansen B, Hwang S, López-Otin C, Virgin HW, Celli J.** 2012. Selective subversion of autophagy complexes facilitates completion of the Brucella intracellular cycle. Cell Host Microbe **11:**33–45. http://dx.doi.org/10.1016/j.chom.2011.12.002.
39. **Zheng YT, Shahnazari S, Brech A, Lamark T, Johansen T, Brumell JH.** 2009. The adaptor protein p62/SQSTM1 targets invading bacteria to the autophagy pathway. J Immunol **183:**5909–5916. http://dx.doi.org/10.4049/jimmunol.0900441.
40. **Matsuzawa T, Kim BH, Shenoy AR, Kamitani S, Miyake M, Macmicking JD.** 2012. IFN-gamma elicits macrophage autophagy via the p38 MAPK signaling pathway. J Immunol **189:**813–818. http://dx.doi.org/10.4049/jimmunol.1102041.
41. **Mostowy S, Sancho-Shimizu V, Hamon MA, Simeone R, Brosch R, Johansen T, Cossart P.** 2011. p62 and NDP52 proteins target intracytosolic Shigella and Listeria to different autophagy pathways. J Biol Chem **286:**26987–26995. http://dx.doi.org/10.1074/jbc.M111.223610.
42. **Cemma M, Kim PK, Brumell JH.** 2011. The ubiquitin-binding adaptor proteins p62/SQSTM1 and NDP52 are recruited independently to bacteria-associated microdomains to target salmonella to the autophagy pathway. Autophagy **7:**341–345. http://dx.doi.org/10.4161/auto.7.3.14046.
43. **Schwab JC, Beckers CJ, Joiner KA.** 1994. The parasitophorous vacuole membrane surrounding intracellular *Toxoplasma gondii* functions as a molecular sieve. Proc Natl Acad Sci U S A **91:**509–513. http://dx.doi.org/10.1073/pnas.91.2.509.
44. **Al-Younes HM, Brinkmann V, Meyer TF.** 2004. Interaction of *Chlamydia trachomatis* serovar L2 with the host autophagic pathway. Infect Immun **72:**4751–4762. http://dx.doi.org/10.1128/IAI.72.8.4751-4762.2004.
45. **Lapaquette P, Bringer MA, Darfeuille-Michaud A.** 2012. Defects in autophagy favour adherent-invasive Escherichia coli persistence within macrophages leading to increased pro-inflammatory response. Cell Microbiol **14:**791–807. http://dx.doi.org/10.1111/j.1462-5822.2012.01768.x.
46. **Romagnoli A, Etna MP, Giacomini E, Pardini M, Remoli ME, Corazzari M, Falasca L, Goletti D, Gafa V, Simeone R, Delogu G, Piacentini M, Brosch R, Fimia GM, Coccia EM.** 2012. ESX-1 dependent impairment of autophagic flux by *Mycobacterium tuberculosis* in human dendritic cells. Autophagy **8:**1357–1370. http://dx.doi.org/10.4161/auto.20881.
47. **Yasir M, Pachikara ND, Bao X, Pan Z, Fan H.** 2011. Regulation of chlamydial infection by host autophagy and vacuolar ATPase-bearing organelles. Infect Immun **79:**4019–4028. http://dx.doi.org/10.1128/IAI.05308-11.
48. **Seto S, Tsujimura K, Horii T, Koide Y.** 2013. Autophagy adaptor protein p62/SQSTM1 and autophagy-related gene Atg5 mediate autophagosome formation in response to Mycobacterium tuberculosis infection in dendritic cells. PLoS One **8:**e86017. http://dx.doi.org/10.1371/journal.pone.0086017.
49. **Eskelinen EL.** 2006. Roles of LAMP-1 and LAMP-2 in lysosome biogenesis and autophagy. Mol Aspects Med **27:**495–502. http://dx.doi.org/10.1016/j.mam.2006.08.005.
50. **Su C, Howe DK, Dubey JP, Ajioka JW, Sibley LD.** 2002. Identification of quantitative trait loci controlling acute virulence in *Toxoplasma gondii*. Proc Natl Acad Sci U S A **99:**10753–10758. http://dx.doi.org/10.1073/pnas.172117099.
51. **Begun J, Lassen KG, Jijon HB, Baxt LA, Goel G, Heath RJ, Ng A, Tam JM, Kuo SY, Villablanca EJ, Fagbami L, Oosting M, Kumar V, Schenone M, Carr SA, Joosten LA, Vyas JM, Daly MJ, Netea MG, Brown GD, Wijmenga C, Xavier RJ.** 2015. Integrated genomics of Crohn's disease risk variant identifies a role for CLEC12A in antibacterial autophagy. Cell Rep **11:**1905–1918. http://dx.doi.org/10.1016/j.celrep.2015.05.045.
52. **Sun Q, Fan W, Chen K, Ding X, Chen S, Zhong Q.** 2008. Identification of Barkor as a mammalian autophagy-specific factor for Beclin 1 and class III phosphatidylinositol 3-kinase. Proc Natl Acad Sci U S A **105:**19211–19216. http://dx.doi.org/10.1073/pnas.0810452105.
53. **Charif H, Darcy F, Torpier G, Cesbron-Delauw MF, Capron A.** 1990. *Toxoplasma gondii*: characterization and localization of antigens secreted from tachyzoites. Exp Parasitol **71:**114–124.
54. **Alaganan A, Fentress SJ, Tang K, Wang Q, Sibley LD.** 2014. Toxoplasma GRA7 effector increases turnover of immunity-related GTPases and contributes to acute virulence in the mouse. Proc Natl Acad Sci U S A **111:**1126–1131. http://dx.doi.org/10.1073/pnas.1313501111.
55. **Taylor S, Barragan A, Su C, Fux B, Fentress SJ, Tang K, Beatty WL, Hajj EL, Jerome M, Behnke MS, White M, Wootton JC, Sibley LD.** 2006. A secreted serine-threonine kinase determines virulence in the eukaryotic pathogen *Toxoplasma gondii*. Science **314:**1776–1780. http://dx.doi.org/10.1126/science.1133643.